International Journal of Pharmaceutics: X 5 (2023) 100170

Contents lists available at ScienceDirect

International Journal of Pharmaceutics: X

journal homepage: www.sciencedirect.com/journal/international-journal-of-pharmaceutics-x

Dual-effects of caffeinated hyalurosomes as a nano-cosmeceutical gel counteracting UV-induced skin ageing

Manal A Elsheikh [a], Passent M.E. Gaafar [b], Mohamed A. Khattab [c], Mohamed Kamal A. Helwah [d], Mohamed H. Noureldin [e], Haidy Abbas [a,*]

[a] Department of Pharmaceutics, Faculty of Pharmacy, Damanhour University, Damanhour, Egypt
[b] Department of Pharmaceutics, Division of Pharmaceutical Sciences, College of Pharmacy, Arab Academy for Science, Technology and Maritime Transport, Alexandria, P.O. Box 1029, Egypt
[c] Department of Cytology and Histology, Faculty of Veterinary Medicine, Cairo University, Cairo 12211, Egypt
[d] Avantic Pharmaceuticals, P.O. Box 12556, Giza, Egypt
[e] Department of Biochemistry, Division of Clinical and Biological Sciences, College of Pharmacy, Arab Academy for Science, Technology and Maritime Transport, Alexandria, P.O. Box 1029, Egypt

ARTICLE INFO

Keywords:
Hyalurosomes
Caffeine
Anti-ageing
UVB
Skin delivery
Cosmeceutical

ABSTRACT

Caffeine (CAF) is a challenging natural bioactive compound with proven antiaging efficacy. However, being hydrophilic hampers its permeation through the skin. Our aim is to develop a novel CAF-loaded nano-cosmeceutical tool counteracting skin photoaging via improving CAF skin permeation using a bioactive nanocarrier. Caffeinated hyalurosomes are novel biocompatible antiaging nanoplatforms designed by immobilization of phospholipid vesicles with a hyaluronan polymer. Physicochemical properties of the selected hyalurosomes formulation showed nano-sized vesicles (210.10 ± 1.87 nm), with high zeta potential (−31.30 ± 1.19 mv), and high encapsulation efficiency (84.60 ± 1.05%). In vitro release results showed outstanding sustained release profile from caffeinated hyalurosomes compared to the CAF-loaded in conventional gel over 24 h. The in-vivo study revealed a photoprotective effect of caffeinated hyalurosomes, reflected from the intact and wrinkling-free skin. Results of biochemical analyses of oxidative stress, pro-inflammatory mediators, and anti-wrinkling markers further confirmed the efficacy of the prepared hyalurosomes compared to the CAF conventional gel. Finally, histopathological examination demonstrated normal histological structures of epidermal layers with minimal inflammatory cell infiltrates in the caffeinated hyalurosomes group compared to the positive control group. Conclusively, caffeinated hyalurosomes successfully achieved enhanced CAF loading and penetration into the skin besides the hydration effect of hyaluronan. Consequently, the developed delivery system presents a promising skin protection nano-platforms via the double effects of both hyaluronan and CAF, hence it guards against skin photodamage.

1. Introduction

Nowadays, cosmeceuticals are denoted as a new breed of products which provides hybrid effects of both cosmetic and pharmaceutical products. Controversial to inert cosmetics, cosmeceuticals mainly contain bioactive ingredients intended to have medicinal benefits in the topical application (Morganti et al., 2021). However, the superiorities of cosmeceuticals are undoubted since they offer a quantifiable skin effect (Amasya et al., 2021). Globally, nearly 40% of any dermatologist's prescription contains cosmeceutical agents. Consequently, there is an increase in the global cosmeceutical market which is driven by higher consumer awareness about maintaining a youthful appearance. That's why there is an increased demand for anti-ageing products. Ageing is the crucial factor that leads to the physical appearance of skin collagen in different ways such as; decreased oil production, decreased elasticity, dry skin, loss of texture, age spots and flabby skin (Sherber, 2014). Diverse elements which can nurture skin ageing that can be either internal or external factors. The internal factors encompass the irreversible process of ageing by time or due to hereditary factors, whereas external ones can augment the internal factors, through exposure to harmful

* Corresponding author at: Department of Pharmaceutics, Faculty of Pharmacy, Damanhour University, Damanhour, El-Bahira, Egypt Post Office, P.O. Box 22511, Damanhour, Egypt.
E-mail address: haidy.abass@pharm.dmu.edu.eg (H. Abbas).

https://doi.org/10.1016/j.ijpx.2023.100170
Received 24 December 2022; Received in revised form 4 February 2023; Accepted 7 February 2023
Available online 10 February 2023

solar ultraviolet radiations (UVR), unhealthy lifestyle and stress (Seleem et al., 2022). In fact, vitamin D synthesis requires moderate exposure to sunlight and UVR (Karna et al., 2008). However, increased UVR exposure has been implicated in pathological conditions due to the imbalance in the production of IL-10 and IL-12 and the activation of reactive oxygen species. This is accompanied, as well, by different processes including the activation of collagenase and elastase enzymes resulting in the breakdown of extracellular matrix molecules as collagen. Such implications lead to premature photoaging and the appearance of wrinkles (Beissert and Loser, 2008; Mostafa et al., 2021; Seleem et al., 2022). Therefore, there is a great need for a topically applied, natural compound offering high photoprotective properties with minimal side effects. Drug delivery via the skin has gained considerable attention as it bypasses the limitations of traditional administration routes. However, the major constraint of current cosmeceutical therapy encompasses less skin penetration and short contact time (Krausz et al., 2014). This urged the need for novel, topically applied drug-loaded nano-delivery systems exhibiting significant therapeutic efficacy. Recently, nanotechnology entered the field of cosmeceuticals and offered numerous advantages (Mu and Sprando, 2010) · This includes improved skin penetration of the active molecules and contact time due to the small particle size and high surface area. In addition, nano-cosmeceuticals offer a controlled release of active molecules thus decreasing the number of topical administrations. Novel nanovesicles like liposomes, ethosomes, transfersomes, glycerosomes and hyalurosomes have shown promising results in dermal drug delivery (Abruzzo et al., 2020). Hyalurosomes (HS) are phospholipid nanovesicles immobilized with hyaluronan polymer which possess specific properties for instance; biocompatibility, gelling capabilities and penetration enhancing ability (El Kechai et al., 2015; Kong et al., 2011). Such features provided higher physical stability with superior loading and retention ability of the loaded cargo (Manca et al., 2015), fostering it to be a commonly used polymer in the cosmetic industry (Avadhani et al., 2017). Also, hyaluronan integration with the vesicle structure can enhance vesicles' contact with the skin surface and hence it offers a longer contact time at the application site (Castangia et al., 2016b; Castangia et al., 2022; Witting et al., 2015).

Moreover, the significant anti-ageing effect of hyaluronan was previously highlighted by several reports owing to its radical scavenging potential, skin repair, wound healing, skin hydration properties and combating skin wrinkling. Various studies confirmed the enhanced activity of drugs loaded in hyalurosomes, for instance; Manca et al.(Manca et al., 2015) have proven the improved antirheumatic potentials of curcumin hyalurosomes. Also, Castangia et al. (Castangia et al., 2016c) have shown a greater protective effect against hydrogen peroxide-induced human keratinocytes damage following treatment with phycocyanin-loaded hyalurosomes. Further, the improved antioxidant activity of liquorice-extract loaded hyalurosomes was also confirmed by Castangia et al.(Castangia et al., 2015).

Nowadays, natural topical bioactive compounds are in greater demand and have shown enhanced activity against certain diseases with lesser side effects. In fact, they have been used for skin, face, nails and lips with promising activity against inflammation, photo-ageing and hair loss. Natural bioactive compounds such as gallic acids, catechins, epicatechins, luteolin, curcumin, quercetin, ascorbic acids, alpha and beta carotene and caffeine are frequently used(Ganesan and Choi, 2016). Caffeine (CAF) (**Supplementary Figs. 1,** 1,3,7-trimethylpurine-2,6-dione), a methyl xanthine alkaloid (molecular weight: 194.2 g/mol) could be not only consumed as a beverage but also used either as a medicine or in cosmetic purposes. It is a central nervous system stimulant that might cause wakefulness and augment mental activity (Jacobson et al., 2022). Several studies have reported the use of caffeine in cosmetology owing to its thermogenic, lipolytic, antioxidant and UVR protective effect (Luo and Lane, 2015; Seleem et al., 2022). It had also been suggested that caffeine-based creams and lotions function as sunscreens as they aid in delaying the photo-ageing process of the skin and hindering the tumors' development after exposure to sunlight (Lu et al., 2007; Michna et al., 2006). Furthermore, it was previously highlighted that after either topical or oral administration, caffeine's protective role was through promoting proline synthesis and accordingly increasing collagen synthesis (Seleem et al., 2022). Moreover, caffeine can regulate protein kinases that sensor any damage in DNA and hence block cell-cycle progression and facilitate DNA repair (Koo et al., 2007; Zhou and Bartek, 2004). Unfortunately, due to caffeine's high hydrophilicity (Log $P = -0.07$), it does not possess the ability to penetrate the skin (Bastianini et al., 2021; Menon et al., 2012). Therefore, plenteous efforts have been made recently and are continuing to enhance the dermal delivery of caffeine (Luo and Lane, 2015). Many reports investigated the development of various nano-delivery systems prepared using organic solvents besides more complex preparations. Different nano-systems have been utilized (Abosabaa et al., 2021) to increase skin penetration of caffeine such as; microemulsion (Sintov and Greenberg, 2014), solid lipid nanoparticles (Algul et al., 2018; Puglia et al., 2016), polymeric nanoparticles developed from polycaprolactone synthetic polymer, (Massella et al., 2018) vesicles (Teaima et al., 2018), or ethoniosomes (Kulicke et al., 2008; Puteri and Ernysagita, 2017). On the other hand, hyalurosomes being modified nanovesicles that could be prepared by the simple, eco-friendly method, free from any organic solvent (Manca et al., 2015) could represent a promising nanoplatform. Therefore, loading CAF in hyalurosomes is anticipated to enhance the skin permeability of CAF providing promising antioxidant and anti-inflammatory effects with lower administration frequency.

Fortunately, the current investigation is the first to evaluate the topical double effects of caffeinated-hyalurosomes as an anti-ageing nano-cosmeceutical gel which enhances the skin penetration and deposition of CAF leading to photoprotection against UVB radiation. A full in vitro investigation of the caffeinated hyalurosomes was performed. Biological evaluation using a rat model was conducted succeeded by biochemical and histological evaluations to confirm both safety and efficacy.

2. Materials and methods

2.1. Materials

Caffeine was obtained from Boehringer Ingelheim (Germany). Phospholipon® 90G (P90G) was obtained from Lipoid GmbH (Ludwigshafen, Germany). Sodium hyaluronate (hyaluronan) (1.5–2 kDa) and Carbopol 940 were purchased from Baoji Guokang Bio-Technology Co., Ltd. (China). Other chemicals used in the study were of analytical grade and were purchased from the El-Nasr Company for Pharmaceutical Chemicals (Cairo, Egypt).

2.2. Preparation of caffeinated hyalurosomes

Caffeinated hyalurosomes **(CAF- HS)** were prepared in accordance with the method adopted by Manca et al. (Manca et al., 2015) with some amendments as presented in Table 1. Briefly, 0.15 or 0.2 g of hyaluronan and 0.2 g of caffeine were dissolved in 10 ml distilled water and stirred for 5 h at room temperature to attain a final polymer solution of 2% *w/v* CAF, following that, the drug-polymer solution was added to 0.6 g of Phospholipon 90G (P90G) and left overnight for hydration. Then, the mixture was stirred for 5 h and sonicated (5 s on and 2 s off for 50 cycles;

Table 1
Composition of blank hyalurosomes (HS_{blank}) and caffeinated hyalurosomes (CAF-HS).

Ingredients	F1	F2	F3	F4
Phospholipon® 90G (%w/v)	6	6	6	6
Hyaluronan (%w/v)	1.5	2	1.5	2
Caffeine (CAF) (%w/v)	–	–	2	2
Water (ml)	10	10	10	10

13 mm of probe amplitude) with a high-intensity ultrasonic probe sonicator (Soniprep 150, MSE Crowley, London, United Kingdom). The abovementioned steps were followed as previously mentioned without the incorporation of CAF to obtain blank hyalurosomes (HS_{blank}). Finally, the prepared formulations were tightly sealed and kept in a refrigerator (4 °C) overnight for stabilization prior to further characterization (Elhalmoushy et al., 2022).

2.3. Preparation of caffeine-conventional gel

A conventional control gel of Carbopol-940 loaded with CAF (CAF-GEL) was prepared for comparison with hyalurosomes. Briefly, 0.5 g of carbopol-940 was dispersed in an aqueous solution containing 2% caffeine. Triethanolamine was thereafter added to adjust the pH to 5.5 for neutralizing the polymer in order to obtain a gel and stabilize the skin's ecological balance. The mixture was mixed with a magnetic stirrer at room temperature and then sonicated to eliminate air bubbles (Elhalmoushy et al., 2022).

2.4. In vitro characterization of HS_{blank} and caffeinated hyalurosomes

2.4.1. Encapsulation efficiency

Ultra-filtration was adopted to determine the percentage encapsulation efficiency (% EE) of CAF. Precisely 2.5 ml aliquots of the prepared caffeinated hyalurosomes formulations were transferred into centrifuge tubes fitted with an ultrafilter (Centrisarts®, MWCO 100000, Sartorius, Bohemia, NY, USA). Tubes were centrifuged for 20 min at 3000 rpm at room temperature (Sigma Laboratory Refrigerated Centrifuge, Model 3 K-30, Germany) (Jain et al., 2009). The amount of CAF in the supernatant was determined spectrophotometrically (UV-1800 240 V, Shimadzu Corporation, Kyoto, Japan) at λ_{max} 273 nm (Abosabaa et al., 2021; Khazaeli et al., 2007). All measurements were conducted in triplicates. The amount of encapsulated CAF was calculated as follows: (Gaafar et al., 2021).

$$\mathbf{EE\%} = \frac{\mathbf{A2 - A1}}{\mathbf{A2}} \times \mathbf{100}$$

Where A1 is the amount of free CAF and A2 is the total amount of CAF in the formulation.

2.4.2. Vesicle size, zeta potential and polydispersity index

The physicochemical properties of both HS_{blank} and caffeinated hyalurosomes were assessed by dynamic light scattering (DLS) technique using Zeta sizer Nano ZS. (Malvern, Instruments Ltd., Malvern, UK). Samples were sonicated (5 min) then dilution was performed for all developed formulations with freshly filtered distilled water (1:100) and measured in triplicates over 10 min (Elsheikh et al., 2018). The vesicle stability was investigated by monitoring the quality attributes of the developed preparation in terms of VS, PDI, ZP and %EE over 3 months at room temperature (25 ± 1 °C).

2.4.3. Rheological studies

The viscosity of the selected caffeinated hyalurosomes and CAF-GEL formulations were investigated using cone and plate Brookfield viscometer (Model DV2T; Brookfield Engineering Laboratories, INC., USA) with a spindle 40 (Elhalmoushy et al., 2022). Samples were subjected to different speed ranging from (8–200 rpm) and the measurements were conducted at room temperature (25 °C ± 2 °C).

2.4.4. Fourier transform-infrared spectroscopy

Fourier transform-infrared spectroscopy (FT-IR) spectra were recorded using an FT-IR spectrometer (Model Cary 630, Agilent Technologies, CT, USA) for each of the caffeinated hyalurosomes component separately (caffeine, Phospholipon® 90G and sodium hyaluronate). In addition, physical mixture and the selected caffeinated hyalurosomes were also investigated. Each sample was scanned over the 4000–400 cm^{-1} wave number region (Elnaggar et al., 2018).

2.4.5. In vitro drug release

In-vitro release profiles of the formulated caffeinated hyalurosomes and CAF either in solution form or loaded in a conventional gel were determined using the dialysis bag method (Abbas et al., 2022; Simsolo et al., 2018). One ml sample of CAF aqueous solution, caffeinated hyalurosomes (**F3 and F4**) and CAF-GEL equivalent to 2% *w/v* CAF were placed in the dialysis bag (Visking®, MWCO 12000–14,000, Serva, USA), tied from both ends, immersed in 100 ml release medium (PBS, pH 5.5) (Abd et al., 2021; Amasya et al., 2021; Iriventi and Gupta, 2020; Simsolo et al., 2018) and continuously shaken at 100 rpm in a thermostatic shaking water bath at 32 ± 0.5 °C (Memmert GmbH, Germany). At pre-determined time intervals (0, 1, 2, 3, 6, 8, 24 h), 2 ml samples were withdrawn from the release medium and compensated by an equal volume of fresh medium to maintain sink conditions. Samples were analyzed spectrophotometrically at λ_{max} 273 nm (Arafa et al., 2020) against a buffer solution as blank. Each experiment was assessed in triplicates (Elsheikh et al., 2018; Gaafar et al., 2021).

2.4.6. Transmission electron microscopy

Transmission electron microscopy (TEM) (JEM-1400; JEOL, Japan) was utilized to examine the morphology of both; the selected HS_{blank} and caffeinated hyalurosomes. Samples diluted with distilled water (1:20) were placed on a copper-coated grid and underwent staining with uranyl acetate saturated solution (1%*w/v*) for 30 s before microscopic investigation. The air-dried samples left a thin film that was examined and photographed (Elhalmoushy et al., 2022).

2.5. In vivo study

2.5.1. Animals

The protocol for the study was approved by the Institutional Animal Care and Use Committee (CU-IACUC) Cairo University, Egypt (Ethical Approval Number CU II F 19–22), and they complied with the Guide for the Care and Use of Laboratory Animals published by the US National Institutes of Health (NIH Publication No. 85–23, revised 2011). The experiment was conducted on the dorsal shaved skin of adult male Wistar rats with a weight range between 180 and 220 g (6–8 weeks old). The animals were kept in plastic cages in a conditioned humidity of 50%–55% and atmosphere at 22 ± 3 °C with 12-h light/dark cycles, and allowed free water access.

2.5.2. UVB exposure test

Skin photo-ageing was induced using a UVB irradiation system (Radiation source peak emission at 302 nm, CL-1000 M; UVP, Upland, CA, USA). The utilized doses of UVB irradiation were 40–80 mJ/cm^2 with 15–30 s exposure time where rats were irradiated with a lamp fixed 5 cm above their position (Abbas et al., 2018). Shaving the dorsal side of the rat occurred 24 h preceding to the experiment.

The treatment was continued for 10 days, where 0.5 g of the prepared formulations (equivalent to 10 mg CAF) was topically applied on the dorsal rat skin one hour before the UVB exposure once daily. (Teaima et al., 2018) Animals were then divided into five groups, each containing 10 rats as follows;

- **Group 1:** Rats were treated with a power-off UV lamp (negative control, non-irradiated control).
- **Group 2**: Rats were exposed to UVB-irradiation for 10 consecutive days (Gilchrest and Yaar, 1992) (positive control, Model-irradiated control)
- **Group 3:** Treatment group where 0.5 g of HS_{blank} was topically applied on the rats' dorsal skin 1 h before the UVB irradiation for a period of 10 days (UV + HS_{blank}).

- **Group 4:** Treatment group where 0.5 g of CAF-GEL was topically applied on the rats' dorsal skin 1 h before the UVB irradiation for a period of 10 day (UV + CAF-GEL).
- **Group 5:** Treatment group where 0.5 g of caffeinated hyalurosomes (CAF-HS) was topically applied on the rats' dorsal skin 1 h before the UVB irradiation for a period of 10 day (Abbas et al., 2022) (UV + CAF-HS).

At the end of the experiment, visual inspection of the dorsal side of the rats' skin was performed where wrinkles was observed macroscopically about 10 days after the initiation of UVB irradiation (Abbas and Kamel, 2020). The animals of each group were sacrificed by the intraperitoneal administration of ketamine overdose then killed using cervical dislocation. The dead animals were delivered to the sanitation companies and disposed according to the official biological waste disposal systems.

The treated skin areas were detached and washed with normal saline twice, then cut into small pieces for homogenization with methanol using a WiseTis® homogenizer (HG-15A, Wertheim, Germany). For complete drug extraction, a sonication was performed in 5 ml methanol for 30 min (Abbas et al., 2018). Finally, CAF determination in samples was analyzed after filtration using a membrane filter (pore size of 0.22 μm) by HPLC system.

2.5.2.1. HPLC assay. The assay of CAF was performed by HPLC (Agilent 1260 series, USA) as previously reported by Khalil et al., (Khalil et al., 2022) at λ_{max} 273 nm (C18, 5 mm, 4.6, 150 mm). The isocratic mobile phase comprised purified distilled water (50% *v*/v) and methanol (50% v/v). The flow rate was 0.9 ml/min at 40 °C. (Hamishehkar et al., 2015; Khalil et al., 2022).

2.5.3. Biochemical analysis

Biochemical measurements were performed 3 days succeeding the last UV irradiation to allow the recovery from any acute UV effects (Abbas et al., 2022). This analysis was conducted in order to assess the antioxidant, anti-inflammatory, and anti-ageing activities of the selected caffeinated hyalurosomes formulation (CAF-$HS_{1.5}$) compared to CAF-GEL and HS_{blank}. Several parameters were determined for instance; ***antioxidant parameters***: enzymatic antioxidants (SOD and CAT) and non-enzymatic antioxidants (GSH, MDA); ***anti-inflammatory* marker**: NF-κB; and ***anti-wrinkling parameters***: neprilysin and elastase.

2.5.4. Histopathological studies

Animals were sacrificed at the end of the experiment. For histological studies, the skin specimens obtained from the dorsal skin of rats were formalin-fixed and embedded in paraffin. Skin samples were mounted in neutral buffered formalin (10%) for 72 h, dehydrated in serial ascending grades of ethanol, cleared in xylene and then infiltrated by synthetic paraplast tissue embedding medium. Five microns thick tissue sections were cut to demonstrate the different skin layers using a rotatory microtome fixed into glass slides. Different stains were used such as hematoxylin and eosin (H&E) as microscopic examination staining standards in addition to Masson's trichrome stain for the determination of collagen fibers contents. Standard procedures for sample fixation and staining process were performed according to Culling(Culling, 1974).

2.5.4.1. Microscopic analysis. A microscopic imaging system operated by using Leica module was utilized for histological analyses. Six non-overlapping random fields for each sample from each group were utterly scanned and examined for obtaining the mean epidermal thickness as well as the area percentage of sub-epidermal collagen fibers in Masson's trichrome stained section according to the method adopted by Kamel et al. (Kamel et al., 2022).

2.6. Statistical analysis

Data were manifested as the mean of triplicate experiments ± SD. Statistical analyses of the data were conducted using a one-way analysis of variance ANOVA test then the Tukey test for multiple comparisons was conducted. The GraphPad Prism® (Version 8) software was used (GraphPad Software, Inc., CA, USA). The differences were considered significant at $P < 0.05$.

3. Results and discussion

This study investigated the application of caffeinated hyalurosomes nanoplatform to augment the permeation and deposition of CAF in skin layers as a protective topical antiaging nanogel.

3.1. Development of blank and caffeinated hyalurosomes

In the current investigation, a novel anti-ageing formulation was elaborated for CAF topical delivery based on the immobilization of phospholipid vesicular structure in the hyaluronan polymer network. The nanogel was prepared in an easy, eco-friendly method without using an organic solvent (Castangia et al., 2016a). Both polymer and drug in a solution were added directly to the phospholipids and left overnight to hydrate and swell slowly. Then, lamellar vesicles were formed spontaneously where the hyaluronan chains can be incorporated within phospholipids bilayers beside the inner core forming immobilized hyalurosomal vesicles. Finally, sonication was adopted for dispersions in order to develop a uniform and small vesicle size (Manca et al., 2015). The key ingredient in hyalurosomes is the hyaluronan polymer which possesses a natural self-gelling, non-irritant nature, beneficial for all skin types and allowing deep penetration in the skin (Jeon et al., 2015; Manca et al., 2015). It should be highlighted that the higher the hyaluronan concentration, the higher the viscosity (Becker et al., 2009; Gupta et al., 2019). Therefore, increasing the concentration of hyaluronan from 1.5% to 2% could successfully lead to a more viscous preparation and hence more skin contact time at the application site (Elhalmoushy et al., 2022). Consequently, this novel caffeinated hyalurosomes was prepared for topical use endowed with effective direct skin contact.

3.2. Physicochemical properties measurements vesicle size, zeta potential and polydispersity index

The results of the quality attribute measurements of HS_{blank}, and caffeinated hyalurosomes (1.5% and 2%) were depicted in Table 2. Concerning the vesicular size, the average size of the prepared

Table 2
Mean Vesicle Size, Zeta Potential, Polydispersity Index and Encapsulation Efficiency of HS_{blank} and caffeinated hyalurosomes (CAF-HS). Measurements are expressed as mean ± SD.

Formulation Code	Vesicle size (nm) ± SD	PDI ± SD	Zeta potential (mV) ± SD	Encapsulation efficiency (%) ± SD
F1 ($HS_{balnk\ 1.5}$[a])	188.31 ± 1.06	0.31 ± 0.05	−42.40 ± 1.25	NA
F2 ($HS_{balnk\ 2}$[b])	220.23 ± 1.09	0.32 ± 0.03	−51.30 ± 1.58	NA
F3 (CAF-$HS_{1.5}$[c])	210.16 ± 1.87	0.20 ± 0.01	−24.30 ± 1.19	84.63 ± 1.05
F4 (CAF-HS_{2}[d])	250.74 ± 1.35	0.23 ± 0.04	−33.10 ± 1.45	81.75 ± 1.58

[a] Empty Hyalurosomes with hyaluronan of 1.5%.
[b] Empty Hyalurosomes with hyaluronan of 2%.
[c] Caffeinated Hyalurosomes with hyaluronan of 1.5% and caffeine concentration of 2%.
[d] Caffeinated Hyalurosomes with hyaluronan of 2% and caffeine concentration of 2%.

caffeinated hyalurosomes appears favorable for the desired objective regarding the UV blocking ability and, hence, more skin protective ability (Xia et al., 2007). In addition, a size range smaller than 300 nm guarantees better drug localization within deep skin layers (Elhalmoushy et al., 2022; Yuan et al., 2022). The increases in sodium hyaluronate concentration in **F2** result in an increase in vesicular size from (220.20 ± 1.09 nm) with respect to **F1** (188.30 ± 1.06 nm) ($p < 0.05$). This may be attributed to the polymer chains that interact with the phospholipids and leads to the formation of larger sizes. This result was in harmony with that previously reported by Castangia et al. (Castangia et al., 2015) who ascribed the increase in the vesicular size in presence of hyaluronic acid polymer adsorbed to the vesicular surface and its intercalation through the phospholipid bilayers. Moreover, CAF loading significantly affected the properties of hyalurosomes by increasing the vesicular size (1.1-Fold) greater than that in the HS_{blank} for both **F1** and **F2** ($p < 0.05$). This effect may be due to the incorporation of CAF in both phospholipid bilayer and hyaluronan besides its ability to be entrapped in the hydrophilic gel-core (Khazaeli et al., 2007). Regarding the ZP, both $HS_{blank\ 1.5}$ and $HS_{blank\ 2}$ showed higher negativity values (−42.40 ± 1.25 and −51.30 ± 1.45 mV respectively) owing to the presence of phosphate group in the phospholipids (Phospholipon 90G) and the anionic nature of sodium hyaluronate. Consequently, these high ZP values can reflect the physical stability and the low tendency for aggregation. It should be noted that these negative ZP values are in harmony with the previously reported work of Abruzzo et al. (Abruzzo et al., 2020). Furthermore, as obvious in Table 2, the higher concentration of the polyanion hyaluronate (2% in F2) resulted in a higher surface negative charge compared to the lower concentration (1.5% in F1) by 1.2-Fold. In addition, caffeine loading leads to a decrease in the negativity of hyalurosomes vesicles by 1.75- and 1.54-folds relative to that in the placebo hyalurosomes (1.5% and 2%) respectively, due to the positive nature of caffeine (pKa = 14) (Khazaeli et al., 2007; Luo and Lane, 2015). This further confirmed the CAF adsorption on the outer layer of hyalurosomes and an ionic interaction that may arise between the positively charged CAF and negatively charged hyalurosomes surface. Such results agreed with previous data reported by Khalil et al., who stated a decrease in the ZP value of CAF-resveratrol bilosomes compared to resveratrol-loaded bilosomes alone (Khalil et al., 2022).

3.3. Caffeine encapsulation efficiency

The retention of the active cargo within the nano-vesicular formulations is one of the crucial properties in their evaluation. The amount of CAF encapsulated in hyalurosomes was determined using the ultrafiltration technique and the results are shown in Table 2. Caffeinated hyalurosomes yielded a high encapsulation efficiency percentage (EE%) of 84.60 ± 1.05 and 81.70 ± 1.58 for F3 and F4 respectively, which are promising results for a hydrophilic drug (CAF). This may be ascribed to the fact that CAF possesses pKa of 14 which will be as a positive ion (Khazaeli et al., 2007) enabling its localization inside the vesicular system showing adequate %EE. Conclusively, the formulation (**F3**) that was composed of (HS: CAF) (1.5: 2%*w/v*) was successfully developed with promising physicochemical attributes; consequently, it was selected for the following investigations. With regard to the vesicles stability during 3 months at (25 ± 1 °C), the analyzed parameters (VS, PDI, ZP and &EE) of $HS_{blank\ 1.5}$ and the selected caffeinated hyalurosomes (CAF-$HS_{1.5}$) were demonstrated in Table 3 and showed non-significant difference during the storage time (variation<10%, $p > 0.05$). It should be noted that the hyalurosomes did not display any decrease in the EE ($p > 0.05$) compared to the initial value before storage. Therefore, it emphasizes the high stability of the developed hyalurosomes. This may be attributed to the gel matrix that formed by hyaluronan on the surface, the core and through the vesicular structure yielding an improved stability of the developed formulation (Zhang et al., 2019).

3.4. Rheological studies

Evaluation of the rheological behavior of topical formulations is considered a pivotal step. Several reports confirmed that hyaluronan chains conformational changes are mainly influenced by the surrounding properties of the solution (pH, ionic strength or temperature) (Kupská et al., 2014). The hyaluronan acidic chains in the current study undergoes substantial ionization at pH >3, forming a network of strong intermolecular interactions with viscoelastic characteristics (Manca et al., 2015)(Elhalmoushy et al., 2022). The rheological testing revealed that, at 100 rpm speed, the viscosity of caffeinated hyalurosomes (737. ± 1.12 cp) was 5-fold higher than that of the CAF-GEL (142.8 ± 2.14 cp) thus, confirming the significantly higher gelation ability of hyaluronan in comparison to Carbopol (Supplementary Fig. 2). Furthermore, investigating the flow behavior of caffeinated hyalurosomes revealed a pseudoplastic or shear-thinning flow at room temperature. This might be attributed to the decreased viscosity of the formulation caused by the increased spindle speed (Mo and Nishinari, 2001). It should be noted that, the pseudoplastic flow behavior is favored since it makes it easier for drugs to diffuse through the gel matrix(Elhalmoushy et al., 2022).

3.5. Fourier transform-infrared spectroscopy

FT-IR analysis was used to verify the characteristic functionalities in all the components of the prepared hyalurosomal formulations (CAF, PG90 and hyaluronan). Physical mixture and caffeinated-hyalurosomes formulation (CAF-HS) were evaluated as well **(**Fig. 1**).** For CAF spectrum, it showed strong vibrational bands at 971 cm-1 that is assigned to the N=C–H deformation vibration. These vibrations occur in the imidazole ring. Strong bands were also observed at 1640 cm-1 and at 1700 cm-1 that are considered to be due to C=O of amide-I asymmetric and symmetric stretching vibrations and at 1539 cm^{-1} corresponds to amide-II. The frequency observed at 740 is assigned to be due to O=C–C bending of the pyrimidine ring (Noor et al., 2018). Phospholipon G 90 (PG90) spectrum was observed where strong sharp peaks appear of the characteristic C—H stretching bands at 2925 cm-1, 2853 cm-1. A stretching band of ester carbonyl group was observed at 1736 cm − 1, and an ester C—O stretching band also recoded at 1252 cm − 1. (Salama

Table 3
Vesicle size, Zeta potential, Polydispersity index and Encapsulation efficiency of blank hyalurosomes and caffeinated hyalurosomes measured during 3 months of storage at 25 ^{0}c. Measurements are expressed as mean ± SD.

Code	Initial				1 Months				3 Months			
	Vesicle size (nm)	PDI	Zeta potential (mv)	EE (%)	Vesicle size (nm)	PDI	Zeta potential (mv)	EE (%)	Vesicle size (nm)	PDI	Zeta potential (mv)	EE (%)
$HS_{blank1.5}$	188.31 ± 1.06	0.31 ±0.05	−42.40 ± 1.25	*	190.34 ±2.51	0.37 ±0.01	−41.80 ±0.91	*	193.46 ±1.21	0.28 ±0.03	−41.30 ±0.40	*
CAF-$HS_{1.5}$	210.16 ± 1.87	0.20 ±0.01	−24.30 ± 1.19	84.63 ± 1.05	213.82 ±1.28	0.30 ±0.04	−22.60 ±1.71	83.60 ± 0.54	217.33 ± 1.72	0.34 ± 0.13	−20.90 ± 1.01	82.71 ± 0.63

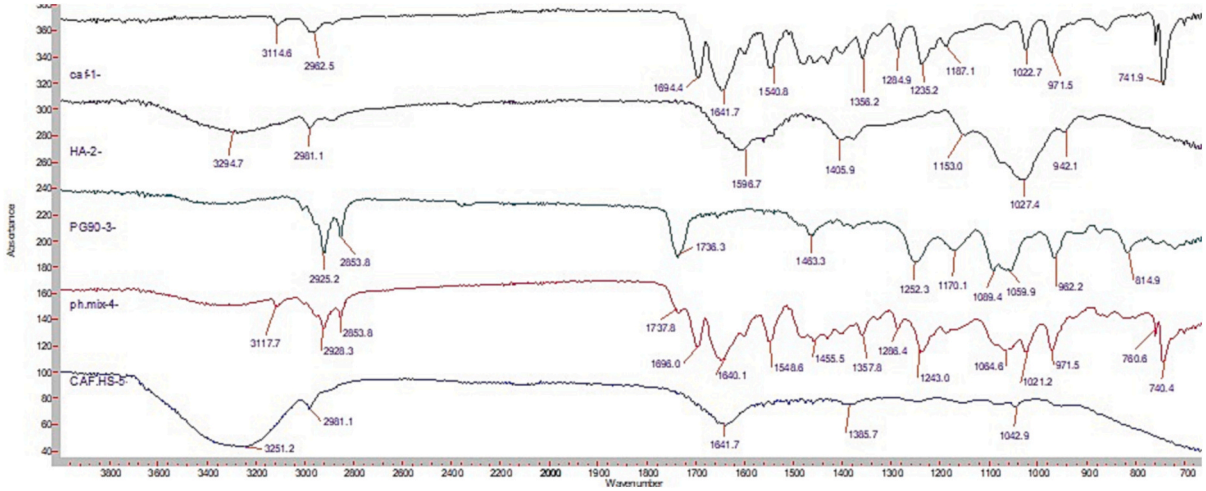

Fig. 1. FT-IR of caffeine, hyaluronan, Phospholipone 90 G, physical mixture and caffeinated hyalurosomes.

et al., 2019). Regarding the hyaluronan spectrum, a broad stretching peak of O–H/N–H bond was observed at 3295. In addition, sharp peaks were observed at 2980, 1596, 1405, and 1027 cm^{-1} that are because of the C—H bond, amide-II, C—O bond of –COONa group, and C–O–C bond, respectively. The peaks at 1376 and 947 cm − 1 are due to the vibrations of C—H bending and C–O–H deformation, respectively(Bang et al., 2017; Manju and Sreenivasan, 2011).

On the other hand, the physical mixture spectrum showed no change in the characteristic peaks of all hyalurosomes components. This indicates the absence of interaction by between them. Finally, Significant spectroscopic changes were observed in FT-IR spectrum of caffeinated-hyalurosomes. The characteristic peaks of IR-spectrum of individual components disappeared when compared to its physical mixture. These observations suggest the presence of a sort of interaction that takes place during hyalurosomes preparation.

3.6. Transmission electron microscopy (TEM)

Microscopical investigation was performed to examine the morphology of the selected HS_{blank} and caffeinated hyalurosomes formulation **(**Fig. 1 **A and B** respectively). TEM micrographs for both formulations revealed; characteristic well-dispersed, spherical, well-separated with no aggregation shell-core vesicles clearly identified with darker coat and core in the case of caffeinated hyalurosomes **(**Fig. 2**B). Such results further confirmed the adsorption of CAF on the vesicular surface and inside the gel core of the hyalurosomes.**

3.7. In vitro release studies

The release behavior of the active cargo from the drug delivery system governs its effectiveness**.** Fig. 3 showed the amount of CAF released from both F3 and F4 hyalurosomal formulations compared to CAF solution and CAF-GEL. Fig. 3 demonstrated that the CAF solution was completely released after 3 h confirming CAF dialyzability.

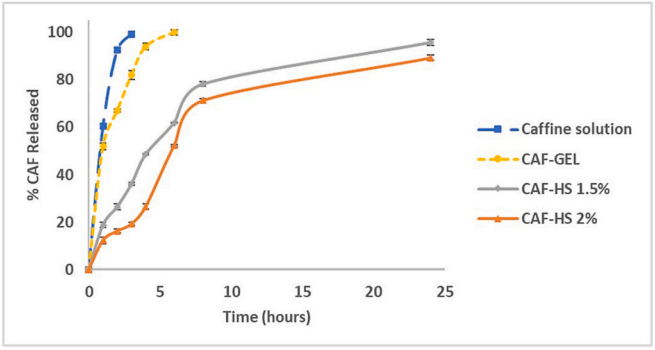

Fig. 3. In vitro release profile of CAF from CAF solution, CAF-GEL and Caffeinated hyalurosomes with different hyaluronan concentrations (1.5% and 2% *w/v*) in phosphate buffer saline (pH 5.5) (CAF concentration equivalent to 2%w/v). Results are represented as mean ± SD, $n = 3$.

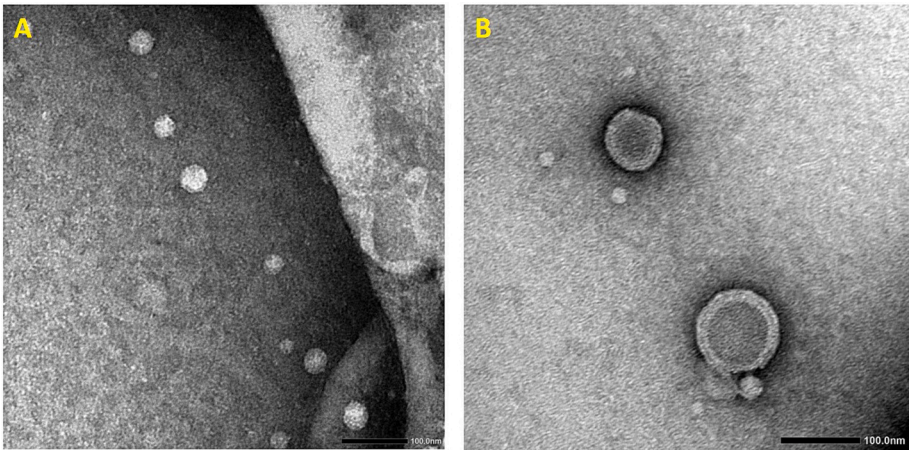

Fig. 2. TEM of (A) HS_{blank} and (B) Caffeinated hyalurosomes (magnification: 50,000× and 60,000× respectively).

Concerning CAF-GEL, the release profile showed a rapid release pattern similar to CAF solution but with more retardation in the release rate (100% released after ~6 h). The slower release rate of CAF-GEL may be ascribed to the required time for the release medium to penetrate into the polymer matrix to allow the diffusion of the CAF into the aqueous release medium. Regarding the caffeinated hyalurosomes, biphasic drug-release patterns were observed from the prepared caffeinated hyalurosomes (1.5% and 2%). Both F3 and F4 formulations showed a gradual burst release pattern of CAF in the first 2 h followed by a prolonged release pattern that continued to 95.8 and 89.3% respectively throughout 24 h. Such sustained release behavior confirmed the efficient encapsulation of CAF in the hyalurosomal system. Therefore, more time was required for CAF partitioning into the release medium from the vesicles which was considered the predominate step in release rather than dissolution. It should be highlighted that F4 showed a more sustained release of CAF from hyalurosomes compared to F3 due to a higher concentration of hyaluronan polymer, this was in good agreement with the previously published work by Gupta et al. (Gupta et al., 2021). It is worth mentioning that, the sustained release behavior of the caffeinated hyalurosomes offers an advantage of greater patient compliance with fewer times of topical applications.

3.8. *In vivo studies*

3.8.1. *UVB exposure test*

Visual examination was assessed for the dorsal skin of the rats after topical pre-application of HS $_{\text{blank 1.5}}$, CAF-GEL and caffeinated hyalurosomes (CAF-HS $_{1.5}$). As obvious in Fig. 4, an intact and smooth skin surface in the non-UV-treated group were revealed. In contrast, edema, signs of erythema and thick skin with notable scars were observed after UV-irradiation in the model group (Fig. 4 **A**). In addition, the thickening of the skin could be seen due to the epidermal hyperplasia and the stratum corneum thickening (Clydesdale et al., 2001). All these signs were lacking in the case of the normal control group (Fig. 4 **B**). On the contrary, pre-application with CAF-GEL (Fig. 4 **C**) resulted in only a few scar traces, whereas the pre-application of HS_{blank} (Fig. 4 **D**), offered a promising protective effect. This result was in good harmony with the previously published study by Manca et al. (Manca et al., 2015), who reported that the empty hyalurosomes exhibited a protective activity due to the presence of phospholipids and besides the intrinsic antioxidant activity of the hyaluronan. In addition, it was reported that hyaluronan can stimulate the production of endogenous hyaluronan thus leading to wound healing process (Elhalmoushy et al., 2022; Jeon et al., 2015). In addition, it has been previously reported that hyaluronan offers advantages of skin hydration, skin repair and protection against skin wrinkling (Avadhani et al., 2017).

On the other hand, after the pre-application of caffeinated hyalurosomes the skin appeared intact and free from any wrinkling signs (Fig. 4 **E**). This synergistic affect was expected because of the better skin penetration of caffeine loaded in the nano-sized hyalurosomes, in addition to the intrinsic activity of hyalurosomes that leads to better skin protection from photodamaging (Luo and Lane, 2015). Consequently, such dual effects allowed overcoming the impermeability obstacles of the outermost layer of the skin and hence offered a promising protective anti-ageing effect.

Regarding CAF deposition in the rat skin Fig. 5, the results showed that the caffeinated hyalurosomes exhibited 4.89-fold higher skin accumulation compared to CAF-GEL. Such results further confirmed the previous findings regarding the increased permeability of the caffeinated hyalurosomes across the stratum corneum barrier after the topical application. Similar findings were reported by EL halmoushy et al., (Elhalmoushy et al., 2022) where berberine-loaded hyalurosomes demonstrated a significant increase in skin retention in comparison to berberine loaded in conventional carbopol gel after 24 h. Therefore, our findings highlighted the ability of HS to encapsulate and retain CAF in deep skin layers which fulfil our aim, therefore, this novel caffeinated hyalurosomes can be used as a potential anti-ageing topical nanogel.

3.8.2. *Biochemical analysis*

Evaluation of different biochemical markers can be used to assess the effect of the pre-application of the different formulations after exposure to UVB irradiation. In the current study, the anticipated prophylactic potential of the prepared caffeinated hyalurosomes was examined by determination of the level of various markers; antioxidant, anti-inflammatory, and anti-wrinkling.

3.8.2.1. Antioxidant markers. Solar radiations (UVA and UVB) induce the formation of reactive oxygen species (ROS) in skin tissues. The latter is controlled by normal cellular regulation mechanisms due to the presence of cellular antioxidants. However, the decrease in cellular homeostasis and the increase in ROS lead to photo-ageing and carcinogenesis. (Avadhani et al., 2017).

The antioxidant potential of the developed caffeinated hyalurosomes was assessed by measuring several markers such as; GSH, MDA, SOD and

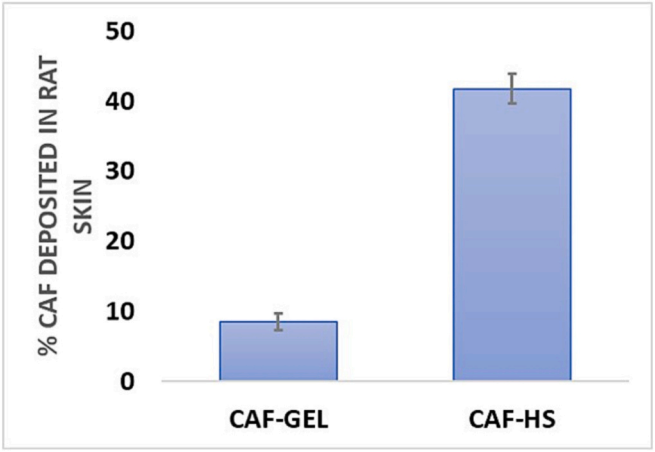

Fig. 5. Skin deposition of CAF in dorsal rat skin after 24 h from the topical application of CAF-GEL and caffeinated hyalurosomes. Results are represented as mean ± SD, n = 3.

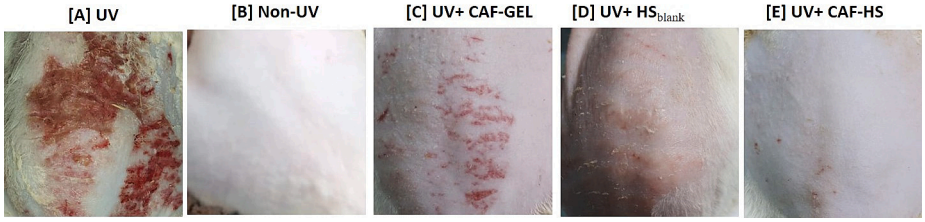

Fig. 4. Pictures of the dorsal skin of rats (A) UVB-irradiated group, (B) Non UVB irradiated group, (C) UVB-irradiated and pretreated topically with 0.5 g CAF-GEL, for 10 days. (D) UVB-irradiated and pretreated topically with 0.5 g HS_{blank} for 10 days.and (E) UVB-irradiated and pretreated topically with 0.5 g caffeinated hyalurosomes for 10 days.

CAT. In the current work, Fig. 6 **(A)** revealed the effect of the tested formulations on enzymatic antioxidants (SOD and CAT) and non-enzymatic antioxidants (GSH, MDA). Upon exposure to solar UV irradiation, the levels of GSH, SOD, and CAT decrease, and the level of MDA level increases (Abbas et al., 2018). Our results confirmed that the model-irradiated group (UVB-irradiated positive control) (**Group II**) showed a statistical difference from the normal control group (negative control) (**Group I**) by 4.23-, 3.69- and 2.80-fold for either CAT, SOD or GSH respectively. On the other hand, the model-irradiated group significantly elevated the level of MDA by 3.7-fold compared with the normal group. This was in good agreement with the previously published data by Raza et al. (Raza et al., 2013) who reported that UV-irradiation induces elevated levels of ROS and lipid peroxidation. Regarding, the topical administration of CAF-GEL (**Group III**), considerable effect in the antioxidant markers' levels compared with the model group was observed, where the ANOVA results revealed significant enhancement in the levels of CAT, SOD, and GSH in the CAF-GEL group compared with the model-irradiated group by 1.29, 1.45, and 1.89-fold, respectively. In addition to, a significant decline in MDA level by 1.51-fold in the CAF-GEL group compared with the model-irradiated group. This by turn verified the antioxidant effect of caffeine. It is previously reported that MDA considered as a crucial biomarker for endogenous DNA damage (Raza et al., 2013). Thus, it can be concluded that CAF presented promising protection against lipid peroxidation.

Fortunately, HS_{blank} showed surprising results where an improvement was recorded in CAT, SOD, and GSH levels in comparison to the model-irradiated group by 1.9-, 1.7-, and 1.4-fold respectively. Besides, HS_{blank} decreased the MDA level by 1.36-fold compared with the model UVB-irradiated group. Such results confirmed the intrinsic activity of the hyalurosomes. Similar results were reported by Elhalmoushy et al., who assessed the biological activity of berberine-loaded hyalurosomes against vitiligo (Elhalmoushy et al., 2022). A synergistic effect was observed in the caffeinated hyalurosomes group where the ANOVA results demonstrated significant improvement in the level of the anti-oxidant markers more than those of CAF-GEL and HS_{blank} collectively when compared to the model UVB-irradiated group. By comparison to the CAF-GEl group, Fig. 6 **A** showed a significant elevation in the levels of CAT, SOD, and GSH by 3.0-, 2.0- and 1.04-fold, respectively. Additionally, caffeinated hyalurosomes decreased the MDA level by 1.56-fold compared with CAF-GEL. Consequently, the developed hyalurosomes gel is a promising nanoplatform for skin delivery of natural antioxidant constituent as CAF. The enhanced antioxidant activity could be attributed to hyaluronan integration with phospholipid vesicle which possesses a radical scavenging potential. These came in harmony with Castangia et al. (Castangia et al., 2016c) who have proven the greater protective effect of phycocyanin-loaded hyalurosomes against damage in human keratinocytes induced by hydrogen peroxide. Also, Castangia et al. (Castangia et al., 2015) have reported the improved antioxidant activity of liquorice extract-loaded hyalurosomes. Moreover, the incorporation of phospholipids could improve skin penetration through

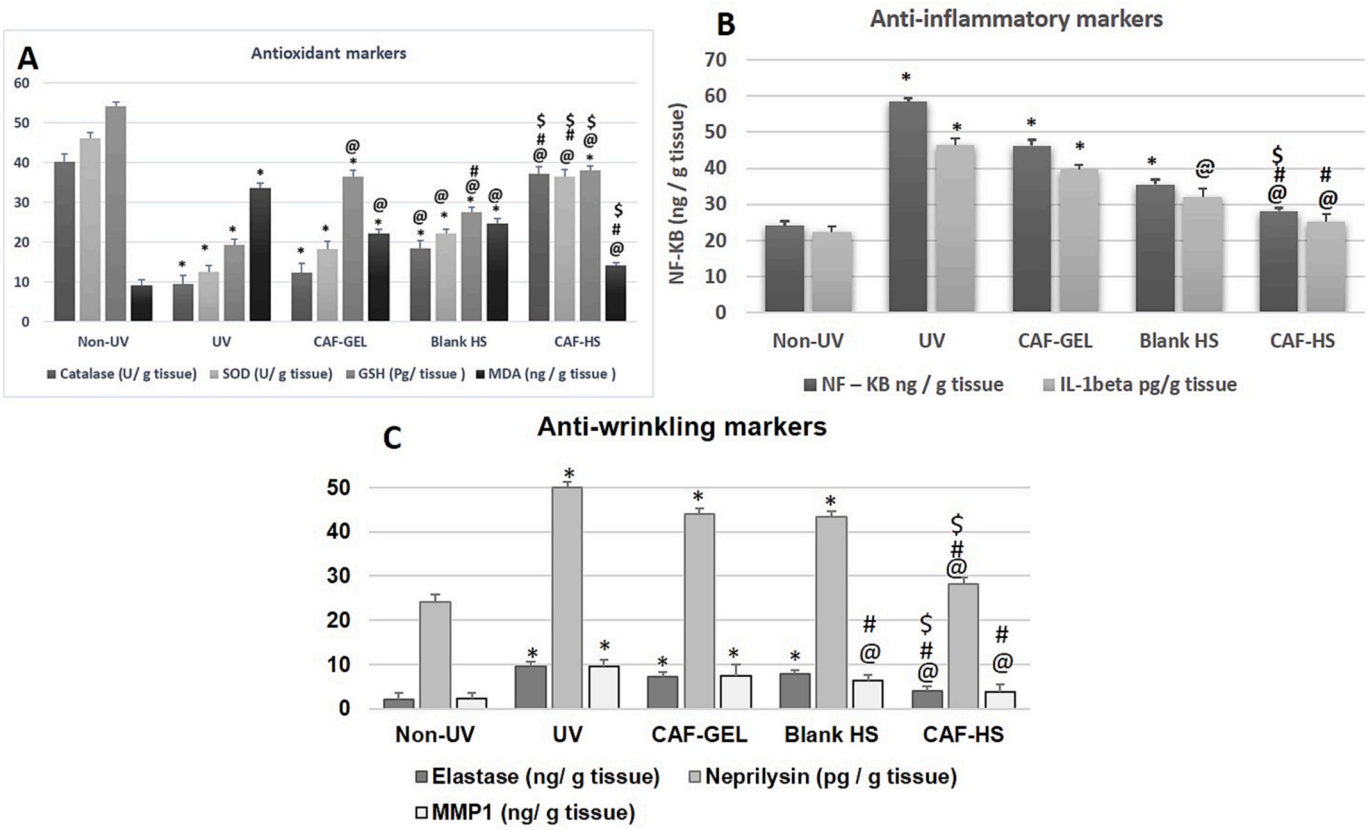

Fig. 6. Biochemical marker evaluation of (A) Anti-inflammatory markers including; catalase, SOD, GSH and MDA levels (B) Anti-inflammatory marker (NF-κB levels) (C) Anti-wrinkling markers including; elastase, and neprilysin levels. Rats were divided into 5 groups (each, $n = 10$) and categorized as following: Non-UVB irradiated group (negative control or normal), model-irradiated group (positive control), CAF-GEL (exposed to UV radiation for 15–30 s radiation first followed by topical administration of 0.5 g CAF-GEL, every day for 10 days), Blank HS (exposed to UV radiation first for 15–30 s followed by topical application of 0.5 g blank HS and caffeinated hyalurosomes (exposed to UV radiation first for 15–30 s followed by topical application of 0.5 g CAF-HS for 10 days). Statistical analyses were conducted using one-way analysis of variance (ANOVA) followed by the Tukey–Kramer post hoc test, whereby each value was presented as mean ± standard deviation (SD). * Statistically significantly different from the non-irradiated negative control group ($P < 0.05$); @ Statistically significantly different from the model-irradiated positive control group ($P < 0.05$); # Statistically significantly different from the CAF-GEL group ($P < 0.05$); $ Statistically significantly different from the blank HS group ($P < 0.05$).

alterations in the SC bilayer structure. Furthermore, the reduced particle size of the developed hyalurosomes enabled them to access the stratum corneum and thereby promoting CAF delivery through the skin. This was in a good agreement with the several reports previously published (Abd et al., 2021; Abruzzo et al., 2020; Castangia et al., 2015) Conclusively, caffeinated hyalurosomes augment the protective and shielding effect of CAF and hence, it can present a potential tool that counteract UVB-induced photo-ageing.

3.8.2.2. Anti-inflammatory markers. It was reported that inhibition of the inflammatory cascade causes a repair against tissue damage (Castangia et al., 2014). Topical application of anti-inflammatory products can substantially restore skin homeostasis and functionality (Castangia et al., 2015; Castangia et al., 2014; Manca et al., 2014; Manca et al., 2015). ELISA was conducted to measure the elevated proinflammatory cytokine level, NF-κB and IL-1β which are associated with the skin damage that induced by UV radiation (Jeon et al., 2014). Fig. 6 **B** demonstrated the effect of the groups under investigation on this proinflammatory cytokines. UVB exposure in the model-irradiated group induced a significant increase in NF-κB by a 2.42-fold and IL-1β by 2.1-fold compared with that of the normal control group ($P < 0.05$). These findings were in accordance with the previously published reports (Abbas et al., 2022; Abbas and Kamel, 2020), which confirmed the elevation of different proinflammatory cytokines after UV irradiation. The inflammatory effect was decreased in the case of pretreatment with CAF-loaded formulations; either CAF-GEL or caffeinated hyalurosomes (**Group III and Group V**). In CAF-GEL, a significant decline in the level of the pro-inflammatory marker NF-κB by 1.26-fold and IL-1β by 1.16-fold relative to the positive control group ($P < 0.05$). This may be attributed to the fact that caffeine belongs to the family of methylxanthines which have known immunomodulatory properties as analogues of adenosine receptors. Such extracellular adenosines are accompanied by cytoprotective functions (Jacobson et al., 2022). CAF non-selectively binds to adenosine receptors in cells of the immune system and hence producing an increase in the anti-inflammatory response which leads to the suppression of the release of pro-inflammatory cytokines (de Alcântara Almeida et al., 2021).

On the other hand, **Group V** (Caffeinated hyalurosomes) showed a significant reduction in NF-κB by 1.64-fold and IL-1β by 1.56-fold compared with **Group III** (CAF-GEL) ($P < 0.05$). The greater effect of the caffeinated hyalurosomes on the inflammatory reactions can be ascribed to the intrinsic properties of the hyalurosomes themselves. As previously mentioned, hyaluronan has been recognized as a promising bioagent for the inflammatory skin diseases for instance; dry skin, hyperplasia, skin erythema, photokeratitis, actinic keratosis, chronic wounds, and others (Chen et al., 2018) (Zhu et al., 2020). Remarkably, no significant difference was displayed between the caffeinated hyalurosomes group and the normal control group. Therefore, the caffeinated hylaurosomes played a superior role in opposing skin photo-ageing. It is worth mentioning that, empty hyalurosomes (HS_{blank}) showed significant ant-inflammatory properties besides their antioxidant activity. Results demonstrated that HS_{blank} decreased the NF-κB by 1.47-fold and IL-1β by 1.45-fold compared to the model group.

3.8.2.3. Anti-wrinkling markers. The cleavage of interstitial collagens and alteration of the extracellular matrix is primarily responsible for the clinical manifestations of skin ageing such as wrinkles and laxity. Thus, inhibition of collagenase was considered a key factor to slow down the loss of elasticity (Imokawa and Ishida, 2015; Wittenauer et al., 2015). As shown in Fig. 6 **C**, the anti-wrinkling markers; elastase, MMP-1 and neprilysin levels were significantly higher in the model-irradiated group compared to the normal control one ($P < 0.05$) by 4.5-, 3.9- and 2.07-fold, respectively. Application CAF-GEL (**Group III**) protected the skin from ageing and wrinkling ($P < 0.05$). This result was in good agreement with the previously published study by Nisakorn Saewan (Saewan, 2022) who confirmed the superior elastase inhibition effect of CAF. Also, Lee et al. (Eun Lee et al., 2019)reported that the inhibition of collagenase occurred in a concentration-dependent manner of CAF. Results of HS_{blank} (**Group IV**) showed significant improvement in the elastase, MMP-1 and neprilysin levels compared to the model group by 1.23-, 1.48- and 1.15-fold respectively, which further supports the previous UVB exposure results. Finally, the caffeinated hyalurosomes offered a superior anti-wrinkling effect that was significantly higher than that of CAF-GEL where it decreased the levels of elastase, MMP-1 and neprilysin by 1.91-, 1.97- and 1.54-folds respectively. This may be attributed to the additive effect of hyaluronan in the developed hyalurosomes which possess skin repair potential and enhance collagen formation and viscoelasticity of the skin. In addition to its intrinsic hygroscopic nature that also promotes the hydration of the skin, lubrication and youthfulness of the skin (Avadhani et al., 2017; Weindl et al., 2004).

3.8.3. Histopathological examination

Microscopic examination of rat skin of normal control samples under light microscopy displayed normal histoarchitecture features of skin layers including apparent intact thin epidermal layers with apparent intact keratinocytes overlaying intact layer of the dermis (Fig. 7 **A, B)** with high records of sub epidermal collagen fibers (up to 41.8% of microscopic field area) (Fig. 8 **A)** with minimal inflammatory cells infiltrates and normal vasculatures. However; in UVB-irradiated group, samples showed marked increase in the thickness of the epidermal layer up to 4.6 folds compared with normal controls. Higher figures of sub-epidermal inflammatory cells infiltrate and congested sub-epidermal small blood vessels **(**Fig. 7 **C, D)**. A significant decrease in the area percentage of collagen fibers in the sub-epidermal zone up to 26.3% than normal control samples was recorded **in** Fig. 8 **B**. CAF-GEL samples (Fig. 7 **E, F)** demonstrated partial protective efficacy with a significant reduction of average epidermal thickness up to 30% compared with model UVB irradiated group samples with milder records of sub-epidermal inflammatory cell infiltrates as well as congested BVs. Moreover; up to 1.1% increases in sub-epidermal collagen fibers were recorded in comparison to model samples (Fig. 8 **C)**. HS_{blank} samples (Fig. 7 **G, H(**showed a more significant decrease of mean epidermal thickness up to 39.5% compared with model UVB irradiated samples with minimal records of abnormal infiltrates or congested vasculatures among all groups. However; insignificant changes were observed in sub-epidermal collagen fibers compared with model samples in most examined samples)Fig. 8 **D(**. Caffeinated hyalurosomes samples (Fig. 7 **I, J**) demonstrated the best-protected group in regard to mean epidermal thickness with up to 68.5% reduction rate compared with model-irradiated samples with sporadic focal records of sub-epidermal infiltrates of congested BVs that were shown in some samples. Moreover, as shown in Fig. 8 **E**, insignificant changes in sub-epidermal collagen fibers density were recorded compared with normal control samples**.**

4. Conclusion

In the present work, caffeinated hyalurosomes were efficiently developed for the first time as an anti-ageing nanoplatform for the delivery of caffeine. The developed nano-delivery system had acceptable particle size, zeta-potential, high encapsulation efficiency and prolonged in-vitro drug release. The in-vivo anti-ageing effect was also examined based on; a UVB exposure test and biochemical analysis quantifying the level of various antioxidant, anti-inflammatory, and anti-wrinkling markers. Caffeinated hyalurosomes showed superior efficacy, thus, the developed formulation offered precious protective anti-ageing effects over either CAF solution or CAF-GEL. In conclusion, caffeinated hyalurosomes showed promising skin penetration and deposition characteristics that should be highly useful as a protective anti-ageing nano-platform.

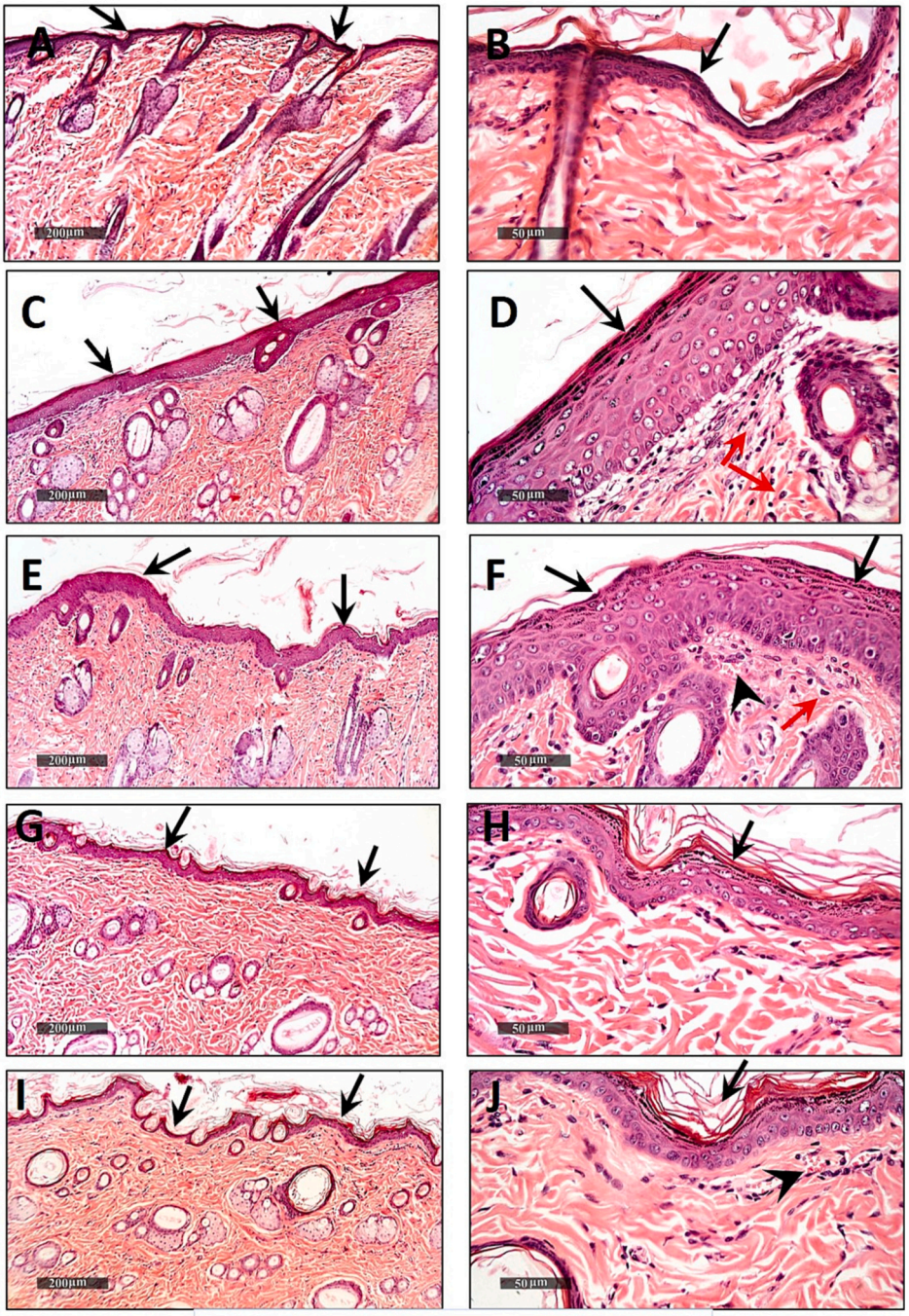

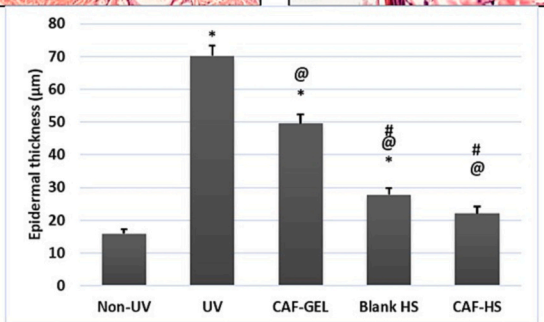

Fig. 7. Micrographs demonstrating histopathological changes in groups under investigation using light microscopy and determination of the mean morphometric analysis of epidermal layer thickness that expressed as mean ± SD * Statistically significantly different from the non-irradiated negative control group ($P < 0.05$); @ Statistically significantly different from the model-irradiated positive control group ($P < 0.05$); # Statistically significantly different from the CAF-GEL group ($P < 0.05$); $ Statistically significantly different from the blank HS group ($P < 0.05$).
Normal control (A&B), Model samples (C&D), CAF-GEL Samples (E&F), HS_{blank} samples (G&H) and caffeinated hyalurosomes samples (I&J). Epidermis (black arrow), inflammatory cells (red arrow) and Congested BVs (arrow head). H&E stain, 100× & 400×. (For interpretation of the references to colour in this figure legend, the reader is referred to the web version of this article.)

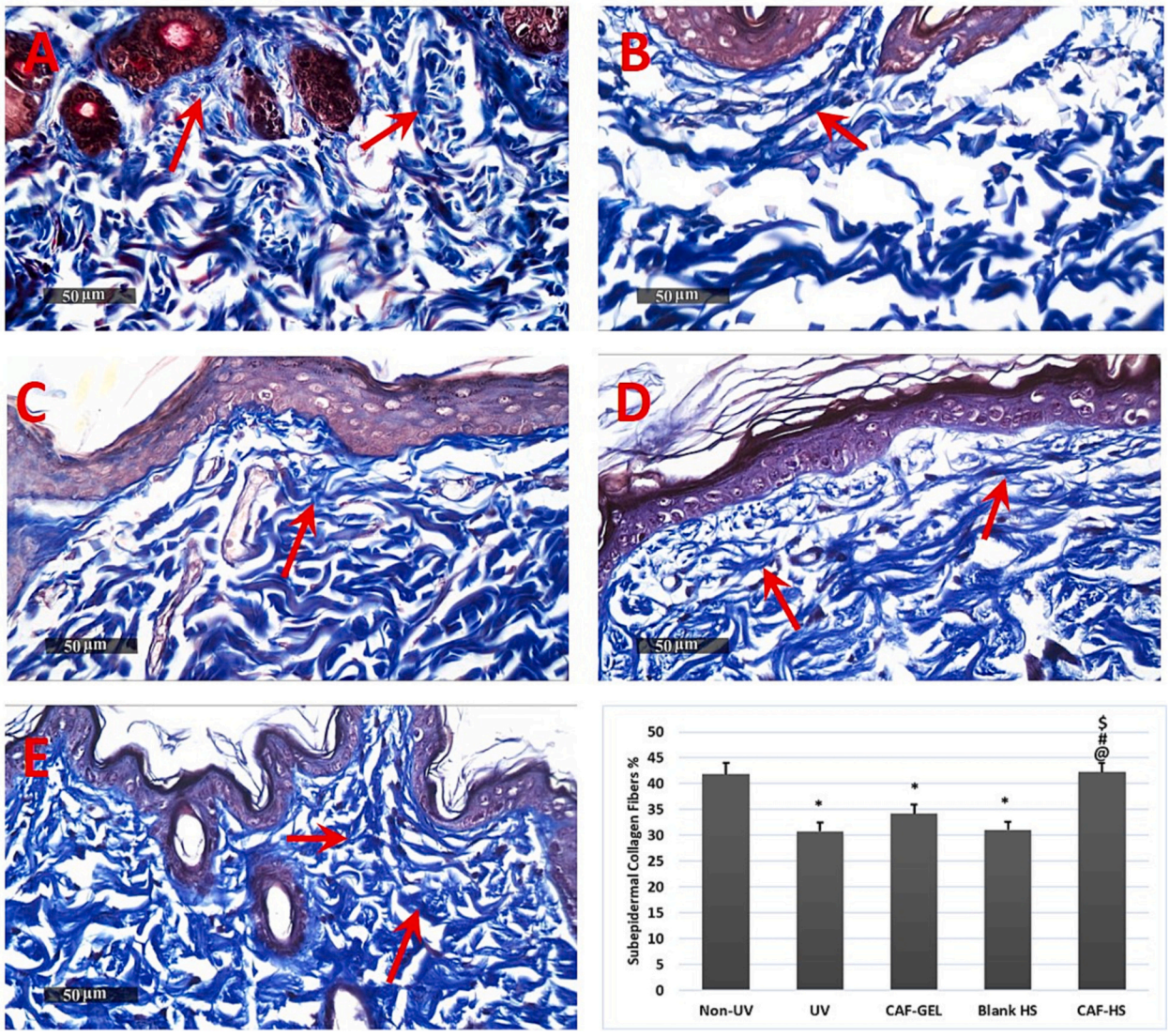

Fig. 8. Histopathological examination of the dorsal rats' skin following Masson Trichrome stain 100×. showing area percentage of sub epidrmal reactive collagen fibers in different groups. Normal control (A), Model samples (B), CAF-GEL Treated Samples (C), HS_{blank} treated samples (D) and caffeinated hyalurosomes treated samples (E). Data were expressed as mean ± SD * Statistically significantly different from the non-irradiated negative control group ($P < 0.05$); @ Statistically significantly different from the model-irradiated positive control group ($P < 0.05$); # Statistically significantly different from the CAF-GEL group ($P < 0.05$); $ Statistically significantly different from the blank HS group ($P < 0.05$).

CRediT authorship contribution statement

Manal A Elsheikh: Conceptualization, Investigation, Methodology, Writing – review & editing, Supervision. **Passent M.E. Gaafar:** Methodology, Investigation, Writing – original draft, Visualization, Data curation, Formal analysis. **Mohamed A. Khattab:** Methodology, Data curation, Writing – original draft, Writing – review & editing. **Mohamed Kamal A. Helwah:** Conceptualization, Resources, Visualization. **Mohamed H. Noureldin:** Investigation, Visualization, Data curation. **Haidy Abbas:** Methodology, Resources, Visualization, Data curation, Supervision.

Declaration of Competing Interest

The authors declare that they have neither conflict of interest nor competing financial interests that could have appeared to influence the work reported in this paper.

Data availability

The authors do not have permission to share data.

Appendix A. Supplementary data

Supplementary data to this article can be found online at https://doi.org/10.1016/j.ijpx.2023.100170.

References

Abbas, H., Kamel, R., 2020. Potential role of resveratrol-loaded elastic sorbitan monostearate nanovesicles for the prevention of UV-induced skin damage. J. Lipos. Res. 30 (1), 45–53.

Abbas, H., Kamel, R., El-Sayed, N., 2018. Dermal anti-oxidant, anti-inflammatory and anti-aging effects of Compritol ATO-based Resveratrol colloidal carriers prepared using mixed surfactants. Int. J. Pharmaceut. 541 (1–2), 37–47.

Abbas, H., El Sayed, N.S., Ali, M.E., Elsheikh, M.A., 2022. Integrated lecithin-bile salt nanovesicles as a promising approach for effective skin delivery of luteolin to improve UV-induced skin damage in Wistar Albino rats. Colloids Surf B, Biointerfac 211112299. https://doi.org/10.1016/j.colsurfb.2021.112299.

Abd, E., Gomes, J., Sales, C.C., Yousef, S., Forouz, F., Telaprolu, K.C., Roberts, M.S., Grice, J.E., Lopes, P.S., Leite-Silva, V.R., 2021. Deformable liposomes as enhancer of caffeine penetration through human skin in a Franz diffusion cell test. Int. J. Cosmet. Sci. 43 (1), 1–10.

Abosabaa, S.A., ElMeshad, A.N., Arafa, M.G., 2021. Chitosan nanocarrier entrapping hydrophilic drugs as advanced polymeric system for dual pharmaceutical and cosmeceutical application: a comprehensive analysis using Box-Behnken design. Polymers 13 (5), 677.

Abruzzo, A., Cappadone, C., Farruggia, G., Luppi, B., Bigucci, F., Cerchiara, T., 2020. Glycyrrhetinic acid liposomes and hyalurosomes on Spanish broom, flax, and hemp dressings to heal skin wounds. Molecules 25 (11), 2558.

Algul, D., Duman, G., Ozdemir, S., Acar, E.T., Yener, G.J.J.C.S., 2018. Preformulation, characterization, and in vitro release studies of caffeine-loaded solid lipid nanoparticles, 69 (3), 165–173.

Amasya, G., Ozturk, C., Aksu, B., Tarimci, N., 2021. QbD based formulation optimization of semi-solid lipid nanoparticles as nano-cosmeceuticals. J. Drug Deliv. Sci. Technol. 66102737.

Arafa, M.G., Mousa, H.A., Afifi, N.N., 2020. Preparation of PLGA-chitosan based nanocarriers for enhancing antibacterial effect of ciprofloxacin in root canal infection. Drug Deliv. 27 (1), 26–39.

Avadhani, K.S., Manikkath, J., Tiwari, M., Chandrasekhar, M., Godavarthi, A., Vidya, S. M., Hariharapura, R.C., Kalthur, G., Udupa, N., Mutalik, S., 2017. Skin delivery of epigallocatechin-3-gallate (EGCG) and hyaluronic acid loaded nano-transfersomes for antioxidant and anti-aging effects in UV radiation induced skin damage. Drug Deliv. 24 (1), 61–74.

Bang, S., Das, D., Yu, J., Noh, I., 2017. Evaluation of MC3T3 cells proliferation and drug release study from sodium hyaluronate-1,4-butanediol diglycidyl ether patterned gel, 7 (10), 328.

Bastianini, M., Sisani, M., Petracci, A., Di Guida, I., Faffa, C., Cardellini, F., 2021. Caffeine vehiculation into alpha-zirconium phosphate: a multifunctional intercalation product and its application for modified topical release. Mater. Adv. 2 (4), 1313–1319. https://doi.org/10.1039/D0MA00729C.

Becker, L.C., Bergfeld, W.F., Belsito, D.V., Klaassen, C.D., Marks, J.G., Shank, R.C., Slaga, T.J., Snyder, P.W., Panel, C.I.R.E., Andersen, F.A., 2009. Final report of the safety assessment of hyaluronic acid, potassium hyaluronate, and sodium hyaluronate. Int. J. Toxicol. 28 (4_suppl), 5–67.

Beissert, S., Loser, K., 2008. Molecular and cellular mechanisms of photocarcinogenesis, 84 (1), 29–34. https://doi.org/10.1111/j.1751-1097.2007.00231.x.

Castangia, I., Nácher, A., Caddeo, C., Valenti, D., Fadda, A.M., Díez-Sales, O., Ruiz-Saurí, A., Manconi, M., 2014. Fabrication of quercetin and curcumin bionanovesicles for the prevention and rapid regeneration of full-thickness skin defects on mice. Acta Biomater. 10 (3), 1292–1300.

Castangia, I., Caddeo, C., Manca, M.L., Casu, L., Latorre, A.C., Díez-Sales, O., Ruiz-Saurí, A., Bacchetta, G., Fadda, A.M., Manconi, M., 2015. Delivery of liquorice extract by liposomes and hyalurosomes to protect the skin against oxidative stress injuries. Carbohydr. Polym. 134657–134663.

Castangia, I., Manca, M.L., Catalán-Latorre, A., Maccioni, A.M., Fadda, A.M., Manconi, M., 2016a. Phycocyanin-encapsulating hyalurosomes as carrier for skin delivery and protection from oxidative stress damage. J. Mater. Sci. Mater. Med. 27 (4), 75. https://doi.org/10.1007/s10856-016-5687-4.

Castangia, I., Manca, M.L., Catalán-Latorre, A., Maccioni, A.M., Fadda, A.M., Manconi, M., 2016b. Phycocyanin-encapsulating hyalurosomes as carrier for skin delivery and protection from oxidative stress damage. J. Mater. Sci. Mater. Med. 27 (4), 75.

Castangia, I., Manca, M.L., Catalán-Latorre, A., Maccioni, A.M., Fadda, A.M., Manconi, M., 2016c. Phycocyanin-encapsulating hyalurosomes as carrier for skin delivery and protection from oxidative stress damage. J. Mater. Sci. Mater. Med. 27 (4), 1–10.

Castangia, I., Manca, M.L., Razavi, S.H., Nácher, A., Díez-Sales, O., Peris, J.E., Allaw, M., Terencio, M.C., Usach, I., Manconi, M., 2022. Canthaxanthin biofabrication, loading in green phospholipid vesicles and evaluation of in vitro protection of cells and promotion of their monolayer regeneration. Biomedicines 10 (1). https://doi.org/10.3390/biomedicines10010157.

Chen, L.H., Xue, J.F., Zheng, Z.Y., Shuhaidi, M., Thu, H.E., Hussain, Z., 2018. Hyaluronic acid, an efficient biomacromolecule for treatment of inflammatory skin and joint diseases: a review of recent developments and critical appraisal of preclinical and clinical investigations. Int. J. Biol. Macromol. 116572–116584.

Clydesdale, G.J., Dandie, G.W., Muller, H.K., 2001. Ultraviolet light induced injury: immunological and inflammatory effects. Immunol. Cell Biol. 79 (6), 547–568.

Culling, C.F.A., 1974. Chapter 26 - preparation, colour maintenance, fixation and storage of specimens. In: Culling, C.F.A. (Ed.), Handbook of Histopathological and Histochemical Techniques (Third Edition). Butterworth-Heinemann, pp. 529–535. https://doi.org/10.1016/B978-0-407-72901-8.50033-0.

de Alcântara Almeida, I., Mancebo Dorvigny, B., Souza Tavares, L., Nunes Santana, L., Vitor Lima-Filho, J., 2021. Anti-inflammatory activity of caffeine (1,3,7-trimethylxanthine) after experimental challenge with virulent Listeria monocytogenes in Swiss mice. Int. Immunopharmacol. 100108090 https://doi.org/10.1016/j.intimp.2021.108090.

El Kechai, N., Bochot, A., Huang, N., Nguyen, Y., Ferrary, E., Agnely, F., 2015. Effect of liposomes on rheological and syringeability properties of hyaluronic acid hydrogels intended for local injection of drugs. Int. J. Pharmaceut. 487 (1–2), 187–196.

Elhalmoushy, P.M., Elsheikh, M.A., Matar, N.A., El-Hadidy, W.F., Kamel, M.A., Omran, G.A., Elnaggar, Y.S., 2022. Novel berberine-loaded hyalurosomes as a promising nanodermatological treatment for vitiligo: Biochemical, biological and gene expression studies. Int. J. Pharmaceut. 615121523.

Elnaggar, Y.S., Elsheikh, M.A., Abdallah, O.Y., 2018. Phytochylomicron as a dual nanocarrier for liver cancer targeting of luteolin: in vitro appraisal and pharmacodynamics. Nanomedicine (London, England) 13 (2), 209–232. https://doi.org/10.2217/nnm-2017-0220.

Elsheikh, M.A., Elnaggar, Y.S., Hamdy, D.A., Abdallah, O.Y., 2018. Novel cremochylomicrons for improved oral bioavailability of the antineoplastic phytomedicine berberine chloride: Optimization and pharmacokinetics. Int. J. Pharmaceut. 535 (1–2), 316–324.

Eun Lee, K., Bharadwaj, S., Yadava, U., Gu Kang, S., 2019. Evaluation of caffeine as inhibitor against collagenase, elastase and tyrosinase using in silico and in vitro approach. J. Enzyme Inhibit. Med. Chem. 34 (1), 927–936. https://doi.org/10.1080/14756366.2019.1596904.

Gaafar, P.M., El-Salamouni, N.S., Farid, R.M., Hazzah, H.A., Helmy, M.W., Abdallah, O. Y., 2021. Pegylated liquisomes: a novel combined passive targeting nanoplatform of L-carnosine for breast cancer. Int. J. Pharmaceut. 602120666.

Ganesan, P., Choi, D.K., 2016. Current application of phytocompound-based nanocosmeceuticals for beauty and skin therapy. Int. J. Nanomedicine 111987-2007. https://doi.org/10.2147/ijn.S104701.

Gilchrest, B., Yaar, M., 1992. Ageing and photoageing of the skin: observations at the cellular and molecular level. Br. J. Dermatol. 127 (S41), 25–30.

Gupta, R.C., Lall, R., Srivastava, A., Sinha, A., 2019. Hyaluronic acid: molecular mechanisms and therapeutic trajectory. Front. Veter. Sci. 192.

Gupta, M.K., Sansare, V.A., Shrivastava, B., Jadhav, S., Gurav, P.J.N.R.J., 2021. Design and evaluation of sesamol loaded hyaluronic acid functionalized phospholipid nanovesicles: DPPH radical scavenging potential assay, 6 (4), 347–351. https://doi.org/10.22034/nmrj.2021.04.004.

Hamishehkar, H., Shokri, J., Fallahi, S., Jahangiri, A., Ghanbarzadeh, S., Kouhsoltani, M., 2015. Histopathological evaluation of caffeine-loaded solid lipid nanoparticles in efficient treatment of cellulite. Drug Dev. Ind. Pharm. 41 (10), 1640–1646. https://doi.org/10.3109/03639045.2014.980426.

Imokawa, G., Ishida, K., 2015. Biological mechanisms underlying the ultraviolet radiation-induced formation of skin wrinkling and sagging I: Reduced skin elasticity, highly associated with enhanced dermal elastase activity, triggers wrinkling and sagging. Int. J. Mol. Sci. 16 (4), 7753–7775.

Iriventi, P., Gupta, N.V., 2020. Topical delivery of curcumin and caffeine mixture-loaded nanostructured lipid carriers for effective treatment of psoriasis. Pharmacogn. Mag. 16 (68), 206.

Jacobson, K.A., Gao, Z.G., Matricon, P., Eddy, M.T., Carlsson, J., 2022. Adenosine A2A receptor antagonists: from caffeine to selective non-xanthines. Br. J. Pharmacol. 179 (14), 3496–3511.

Jain, V., Nath, B., Gupta, G.K., Shah, P.P., Siddiqui, M.A., Pant, A.B., Mishra, P.R., 2009. Galactose-grafted chylomicron-mimicking emulsion: evaluation of specificity against HepG-2 and MCF-7 cell lines. J. Pharm. Pharmacol. 61 (3), 303–310.

Jeon, I.H., Kim, H.S., Kang, H.J., Lee, H.-S., Jeong, S.I., Kim, S.J., Jang, S.I., 2014. Anti-inflammatory and antipruritic effects of luteolin from Perilla (P. frutescens L.) leaves. Molecules (Basel, Switzerland) 19 (6), 6941–6951. https://doi.org/10.3390/molecules19066941.

Jeon, S., Yoo, C.Y., Park, S.N., 2015. Improved stability and skin permeability of sodium hyaluronate-chitosan multilayered liposomes by Layer-by-Layer electrostatic deposition for quercetin delivery. Colloids Surf. B: Biointerfaces 1214–1297.

Kamel, R.A., Teiama, M.S., El-Hagrassi, A.M., Elgayed, S.H., Khattab, M.A., El-Sayed, E. K., Ibrahim, M.T., Mady, M.S., Moharram, F.A., 2022. Appraisal on the wound healing potential of deverra tortuosa DC. and Deverra triradiata hochst essential oil nanoemulsion topical preparation. Front. Pharmacol. 13940988. https://doi.org/10.3389/fphar.2022.940988.

Karna, E., Miltyk, W., Surażyński, A., Pałka, J.A., 2008. Protective effect of hyaluronic acid on interleukin-1-induced deregulation of β1-integrin and insulin-like growth factor-I receptor signaling and collagen biosynthesis in cultured human chondrocytes. Mol. Cell. Biochem. 308 (1), 57–64.

Khalil, L.M., Abdallah, O.Y., Elnaggar, Y.S.R., El-Refaie, W.M., 2022. Novel dermal nanobilosomes with promising browning effect of adipose tissue for management of obesity. J. Drug Deliv. Sci. Technol. 74103522 https://doi.org/10.1016/j.jddst.2022.103522.

Khazaeli, P., Pardakhty, A., Shoorabi, H., 2007. Caffeine-loaded niosomes: characterization and in vitro release studies. Drug Deliv. 14 (7), 447–452.

Kong, M., Chen, X.G., Kweon, D.K., Park, H.J., 2011. Investigations on skin permeation of hyaluronic acid based nanoemulsion as transdermal carrier. Carbohydr. Polym. 86 (2), 837–843.

Koo, S.W., Hirakawa, S., Fujii, S., Kawasumi, M., Nghiem, P., 2007. Protection from photodamage by topical application of caffeine after ultraviolet irradiation. Br. J. Dermatol. 156 (5), 957–964.

Krausz, A., Gunn, H., Friedman, A., 2014. The basic science of natural ingredients. J Drugs Dermatol 13 (8), 937–943.

Kulicke, W.M., Meyer, F., Bingöl, A.Ö., Lohmann, D., 2008. Visco-elastic properties of sodium hyaluronate. Solutions. 1027 (1), 585–587. https://doi.org/10.1063/1.2964773.

Kupská, I., Lapčík, L., Lapčíková, B., Žáková, K., Juříková, J., 2014. The viscometric behaviour of sodium hyaluronate in aqueous and KCl solutions. Colloids Surf. A Physicochem. Eng. Asp. 45432-37 https://doi.org/10.1016/j.colsurfa.2014.04.018.

Lu, Y.-P., Lou, Y.-R., Xie, J.-G., Peng, Q.-Y., Zhou, S., Lin, Y., Shih, W.J., Conney, A.H., 2007. Caffeine and caffeine sodium benzoate have a sunscreen effect, enhance UVB-induced apoptosis, and inhibit UVB-induced skin carcinogenesis in SKH-1 mice. Carcinogenesis 28 (1), 199–206.

Luo, L., Lane, M.E., 2015. Topical and transdermal delivery of caffeine. Int. J. Pharmaceut. 490 (1–2), 155–164.

Manca, M.L., Castangia, I., Caddeo, C., Pando, D., Escribano, E., Valenti, D., Lampis, S., Zaru, M., Fadda, A.M., Manconi, M., 2014. Improvement of quercetin protective effect against oxidative stress skin damages by incorporation in nanovesicles. Colloids Surf. B: Biointerfaces 123566–123574.

Manca, M.L., Castangia, I., Zaru, M., Nácher, A., Valenti, D., Fernàndez-Busquets, X., Fadda, A.M., Manconi, M., 2015. Development of curcumin loaded sodium hyaluronate immobilized vesicles (hyalurosomes) and their potential on skin inflammation and wound restoring. Biomaterials 71100–71109.

Manju, S., Sreenivasan, K., 2011. Conjugation of curcumin onto hyaluronic acid enhances its aqueous solubility and stability. J. Colloid Interface Sci. 359 (1), 318–325. https://doi.org/10.1016/j.jcis.2011.03.071.

Massella, D., Celasco, E., Salaün, F., Ferri, A., Barresi, A.A., 2018. Overcoming the limits of flash nanoprecipitation: Effective loading of hydrophilic drug into polymeric nanoparticles with controlled structure. Polymers 10 (10), 1092.

Menon, G.K., Cleary, G.W., Lane, M.E., 2012. The structure and function of the stratum corneum. Int. J. Pharmaceut. 435 (1), 3–9.

Michna, L., Wagner, G.C., Lou, Y.-R., Xie, J.-G., Peng, Q.-Y., Lin, Y., Carlson, K., Shih, W. J., Conney, A.H., Lu, Y.-P., 2006. Inhibitory effects of voluntary running wheel exercise on UVB-induced skin carcinogenesis in SKH-1 mice. Carcinogenesis 27 (10), 2108–2115.

Mo, Y., Nishinari, K., 2001. Rheology of hyaluronan solutions under extensional flow. Biorheology 38 (5–6), 379–387.

Morganti, P., Morganti, G., Gagliardini, A., Lohani, A., 2021. From cosmetics to innovative cosmeceuticals—non-woven tissues as new biodegradable carrier, 8 (3), 65. https://doi.org/10.3390/cosmetics8030065.

Mostafa, E.S., Maher, A., Mostafa, D.A., Gad, S.S., Nawwar, M.A., Swilam, N., 2021. A unique acylated flavonol glycoside from Prunus persica (L.) var. florida prince: a new solid lipid nanoparticle cosmeceutical formulation for skincare. Antioxidants 10 (3), 436.

Mu, L., Sprando, R.L., 2010. Application of nanotechnology in cosmetics. Pharm. Res. 27 (8), 1746–1749.

Noor, N., Shah, A., Gani, A., Gani, A., Masoodi, F.A., 2018. Microencapsulation of caffeine loaded in polysaccharide based delivery systems. Food Hydrocoll. 82312-321 https://doi.org/10.1016/j.foodhyd.2018.04.001.

Puglia, C., Offerta, A., Tirendi, G.G., Tarico, M.S., Curreri, S., Bonina, F., Perrotta, R.E., 2016. Design of solid lipid nanoparticles for caffeine topical administration. Drug Deliv. 23 (1), 36–40.

Puteri, A.W., Ernysagita, E., 2017. Penetration test of caffeine in ethosome and desmosome gel using an in vitro method. Int. J. Appl. Pharmaceut. 9120–9123.

Raza, K., Singh, B., Singla, N., Negi, P., Singal, P., Katare, O.P., 2013. Nano-lipoidal carriers of isotretinoin with anti-aging potential: formulation, characterization and biochemical evaluation. J. Drug Target. 21 (5), 435–442.

Saewan, N., 2022. Effect of Coffee Berry Extract on Anti-Aging for Skin and Hair—in Vitro Approach. Cosmetics 9 (3), 66.

Salama, A., Badran, M., Elmowafy, M., Soliman, G.M., 2019. Spironolactone-loaded LeciPlexes as potential topical delivery systems for female acne: in vitro appraisal and ex vivo skin permeability studies. Pharmaceutics 12 (1). https://doi.org/10.3390/pharmaceutics12010025.

Seleem, M., Abulfadl, Y., Hoffy, N., Lotfy, N.M., Ewida, H.A., 2022. Promising role of topical caffeine mesoporous gel in collagen resynthesis and UV protection through proline assessment. Future J. Pharmaceut. Sci. 8 (1), 1–11.

Sherber, N.S., 2014. Topicals in skin rejuvenation: prescription topicals. Fac. Plast. Surgery 30 (01), 012–015.

Simsolo, E.E., Eroğlu, İ., Tanrıverdi, S.T., Özer, Ö., 2018. Formulation and evaluation of organogels containing hyaluronan microparticles for topical delivery of caffeine. AAPS PharmSciTech 19 (3), 1367–1376.

Sintov, A.C., Greenberg, I., 2014. Comparative percutaneous permeation study using caffeine-loaded microemulsion showing low reliability of the frozen/thawed skin models. Int. J. Pharmaceut. 471 (1–2), 516–524.

Teaima, M.H., Abdelhalim, S.A., El-Nabarawi, M.A., Attia, D.A., Helal, D.A., 2018. Non-ionic surfactant based vesicular drug delivery system for topical delivery of caffeine for treatment of cellulite: design, formulation, characterization, histological anti-cellulite activity, and pharmacokinetic evaluation. Drug Dev. Ind. Pharm. 44 (1), 158–171. https://doi.org/10.1080/03639045.2017.1386206.

Weindl, G., Schaller, M., Schäfer-Korting, M., Korting, H., 2004. Hyaluronic acid in the treatment and prevention of skin diseases: molecular biological, pharmaceutical and clinical aspects. Skin Pharmacol. Physiol. 17 (5), 207–213.

Wittenauer, J., Mäckle, S., Sußmann, D., Schweiggert-Weisz, U., Carle, R., 2015. Inhibitory effects of polyphenols from grape pomace extract on collagenase and elastase activity. Fitoterapia 101179–101187.

Witting, M., Boreham, A., Brodwolf, R., Vavrova, K., Alexiev, U., Friess, W., Hedtrich, S., 2015. Interactions of hyaluronic acid with the skin and implications for the dermal delivery of biomacromolecules. Mol. Pharm. 12 (5), 1391–1401.

Xia, Q., Saupe, A., Müller, R.H., Souto, E.B., 2007. Nanostructured lipid carriers as novel carrier for sunscreen formulations. Int. J. Cosmet. Sci. 29 (6), 473–482. https://doi.org/10.1111/j.1468-2494.2007.00410.x.

Yuan, M., Niu, J., Xiao, Q., Ya, H., Zhang, Y., Fan, Y., Li, L., Li, X., 2022. Hyaluronan-modified transfersomes based hydrogel for enhanced transdermal delivery of indomethacin. Drug Deliv. 29 (1), 1232–1242.

Zhang, Y., Xia, Q., Li, Y., He, Z., Li, Z., Guo, T., Wu, Z., Feng, N., 2019. CD44 assists the topical anti-psoriatic efficacy of curcumin-loaded hyaluronan-modified ethosomes: a new strategy for clustering drug in inflammatory skin. Theranostics 9 (1), 48–64. https://doi.org/10.7150/thno.29715.

Zhou, B.-B.S., Bartek, J., 2004. Targeting the checkpoint kinases: chemosensitization versus chemoprotection. Nat. Rev. Cancer 4 (3), 216–225.

Zhu, J., Tang, X., Jia, Y., Ho, C.-T., Huang, Q., 2020. Applications and delivery mechanisms of hyaluronic acid used for topical/transdermal delivery–a review. Int. J. Pharmaceut. 578119127.